excited state of hydrogen must under certain conditions result in appreciable scattering.

Bates[5] has suggested the possibility of dual peaks in charge-transfer cross sections arising from pseudocrossing of potential energy surfaces.

*Work supported in part by the U. S. Army Research Office (Durham) and the U. S. Office of Naval Research.

[1]J. B. H. Stedeford and J. B. Hasted, Proc. Roy. Soc. (London) A227, 466 (1955); R. H. Hughes, J. L. Philpot, J. G. Dodd, and S. Lin, Technical Report, Contract AF19(604)-4966, University of Arkansas, September, 1962 (unpublished).

[2]G. H. Dunn, R. Geballe, and D. Pretzer, Phys. Rev. 128, 2200 (1962).

[3]R. T. Brackmann, W. L. Fite, and K. E. Hagen, Rev. Sci. Instr. 29, 125 (1958).

[4]F. P. Ziemba, G. J. Lockwood, G. H. Morgan, and E. Everhart, Phys. Rev. 118, 1552 (1960).

[5]D. R. Bates, Proc. Roy. Soc. A257, 22 (1960).

LASER BEAM INDUCED ELECTRON EMISSION

David Lichtman and J. F. Ready
Honeywell Research Center, Hopkins, Minnesota
(Received 8 March 1963)

Sharp pulses of electron emission have been observed emanating from the target used in studying beam-surface interaction in vacuum. As part of a program studying the effects of beam-induced gas desorption in ultrahigh vacuum, experiments were performed using focused laser beams on "dag"-coated metal targets. The "dag" used is colloidal carbon in isopropyl alcohol and organic (glycol) binder. While monitoring the gas desorption processes, effects were observed which indicated the emission of an electron current from the target during application of the laser beam. The magnitude of the current was considerable, and its appearance in time relative to the laser pulse was extremely rapid. Experiments were performed to determine quantitatively the magnitude of the electron pulse as well as its shape. The experimental system is shown in Fig. 1.

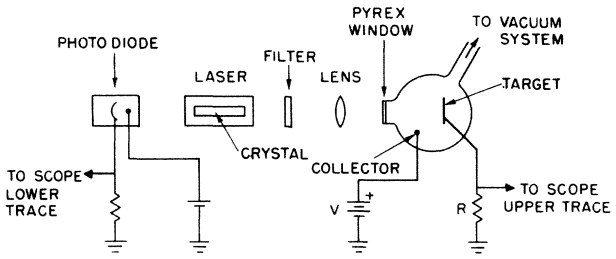

FIG. 1. Configuration of experimental setup. Laser output is obtained from both ends of the laser crystal providing simultaneous signals for photodetector and target bombardment. Measurements were also taken with the oscilloscope probe connected to the collector. The vacuum system is ion-pumped.

In the preliminary experiments, a ruby laser produced a total output pulse of approximately one joule over a total pulse length of approximately 800 microseconds. The output of the laser was focused with a simple lens onto the target, providing a target spot size of approximately 10^{-3} cm^2. Suitable filters were used to insure that only the 1.78-eV photons were being transmitted to the target. A typical laser output and current pulse output are shown in Fig. 2. The very rapid fall-off of current pulses after the first 150 μsec of laser output is not well un-

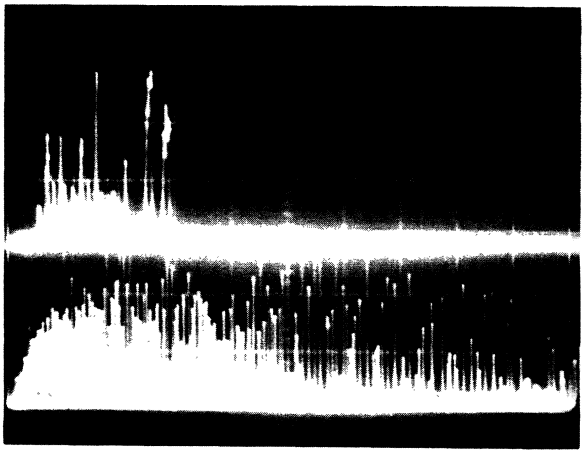

FIG. 2. Scope traces showing electron emission due to absorption of ruby laser beam by carbon target. Lower trace is output of ruby laser. Time scale is 50 μsec/cm. Upper trace shows electron emission pulses. Amplitude scale corresponds to 20 mA/cm. Collector is positive with respect to the target.

derstood but may be due to absorption of subsequent laser pulses in the cloud of evaporated tar-target material which must exist just in front of the target. The extremely sharp electron pulses gave the impression of photoresponse. Field emission could be ruled out since, at optical frequencies, the field does not act in one direction long enough to free electrons from the target material. The possibility of a multiple-photon mechanism was considered, especially since the theoretical calculations of Smith[1] indicate the plausibility of an appreciable photocurrent with focused laser beams. However, we are here considering a material whose work function is approximately 4.5 eV and which would therefore require at least a 3-photon photoelectric effect which is quite unlikely. Since it was possible that we were in some way reducing the work function of the material, measurements were made in an attempt to distinguish between thermionic and multiple-photon emission. The focusing lens was moved and the current pulse output recorded. When the lens was moved about 10% of the focal distance, the electron output decreased by a factor of 10^7. Under these conditions the full laser beam was striking the target under slightly defocused conditions. A change in maximum temperature by a factor of 2 could cause a change in thermionic emission by a factor of 10^7.

Further experiments were done with a neodymium-doped glass rod. This laser provides 1.2-eV photons. Similar results were obtained on the carbon target as seen in Fig. 3. The neodymium laser generated a small number of well-spaced pulses, making it easier to observe the electron-emission pulses. One can easily see the very rapid onset of electron emission coupled with a pulse width that is not more than one microsecond. Further testing of the basic mechanism was pursued by applying the neodymium laser pulse to a tungsten target. The results were identical in form to those obtained with the carbon target. The magnitude of the emission obtained from tungsten was in the order of 50 to 100 milliamperes corresponding to an emission density of 50 to 100 A/cm^2. Consideration of thermionic emission would indicate a surface temperature of the tungsten of about 3300°K.[2] A photoelectric mechanism in this experiment would require four photons of 1.2-eV energy to overcome the tungsten work function of about 4.5 eV.

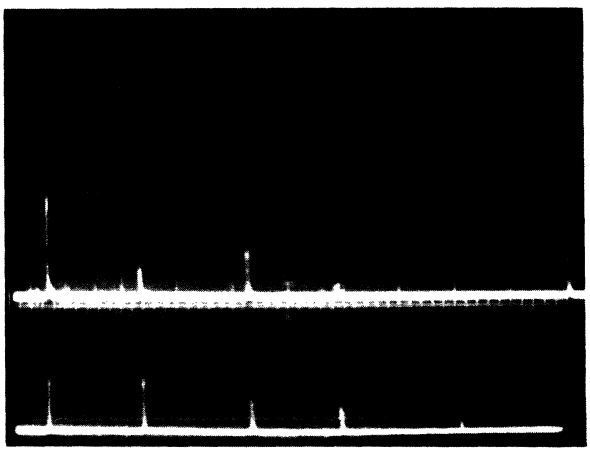

FIG. 3. Results of absorption of neodymium laser beam by carbon target. Lower trace shows output of the laser at 20 μsec/cm. Upper trace shows electron emission pulses. Amplitude calibration is 2 mA/cm. Collector is positive with respect to the target.

In order to estimate the probable temperature of the target surface as a function of time, calculations were made for the application of a single sharp laser pulse.

The temperature of the surface of the carbon was calculated by solving the differential equation for linear heat flow when heat is produced in a thin layer near the surface at the rate of $\alpha F(t)e^{-\alpha x}$ by the laser radiation.[3] Here $F(t)$ is the power density in the focused laser beam at the surface of the carbon, α is the absorption coefficient, and x is the distance from the surface. The calculation was carried out under the assumptions that the power radiated from the surface is negligible compared to input power and conduction losses, that the transverse dimensions of the spot of laser light are large compared to the other dimensions involved, and that the thermal properties of the carbon are those of bulk graphite and are not strongly varying functions of temperature. These assumptions seem reasonable under the conditions used here. The power density was determined with a knowledge of the energy contained in a spike, the time history of the spike, and the area of the target which is irradiated. The temperature of the surface of the carbon target (initially at room temperature) calculated when one spike of the neodymium laser radiation is incident on it is shown in Fig. 4, curve A. The extremely sharp, high-peak-power spikes produced by this laser produce a very rapid heating of the small spot where the laser radiation is focused. Temperatures of several thousand degrees centigrade are reached in a fraction of a microsecond. The observed emission of a plume

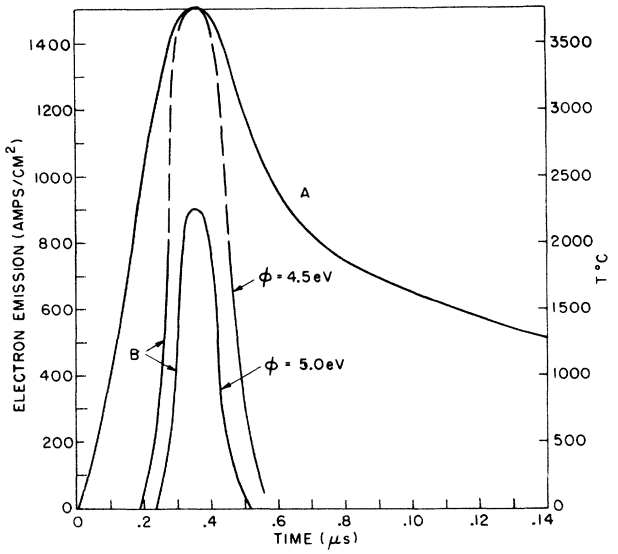

FIG. 4. Curve *A* is the calculated plot of surface temperature as a function of time for the application of a single neodymium laser pulse. Curve *B* is the calculated plot of thermionic electron emission as a function of time for the temperatures indicated in curve *A* and for surfaces of work function 4.5 eV and 5.0 eV.

of vaporized material from the surface of the target confirms the prediction of high temperatures. As the laser pluse ends, thermal conduction causes a rapid decrease in the temperature.

Assuming a work function of approximately 4.5 eV, we have a calculated thermionic emission vs time as shown in Fig. 4, curve *B*. These data indicate that one can observe a thermionic emission pulse in which 99% of the emission occurs over a duration of less than 1 microsecond. Thus one can account for the observation of exceedingly sharp electron pulses corresponding to the application of the laser pulse. The requirements are for temperature rise and fall rates of the order of 10^{10} degrees K per second. The data observed from the application of the ruby-laser pulses on carbon indicate that the temperature of the surface fluctuates by many hundreds of degrees within fractional microsecond intervals.

A further confirmation of our explanation was obtained by reversing the polarity of the voltage applied to the collector electrode so that the target was positive with respect to the collector. The pulses of electron current reaching the collector then disappear. Under these conditions we observed electron pulses arriving at the target, of much smaller amplitude, however, than those obtained from the target in the previous

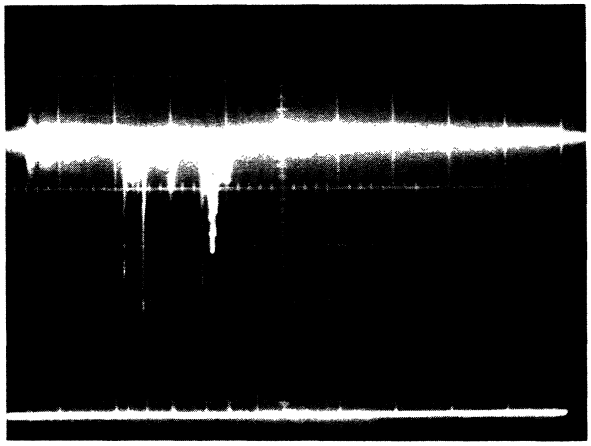

FIG. 5. Results of absorption of neodymium laser beam by the carbon target with the collector held negative with respect to the target. The time scale is 100 μsec/cm. The lower trace indicates the output of the laser. The upper trace indicates electrons arriving at the target. Amplitude scale is 100 μA/cm.

experiments. These pulses are shown in Fig. 5 and may be tentatively explained as follows. The laser beam strikes the target causing the surface temperature to rise to several thousand degrees. The target thus emits radiation, with sufficient high-frequency photons to cause conventional photoelectric emission at the collector electrode. These photoelectrons are then attracted to the target by the applied electric field causing the electron pulses observed. The sharp pulses observed here again indicate the rapid rise and fall of the target temperature.

The results obtained indicate that very high-current-density electron pulses (hundreds of A/cm^2) of extremely short pulse width (0.1 to 1 μsec) can be generated when suitable targets are struck by a focused laser beam. The temperatures and thermionic emission predicted theoretically are very closely approached in the experiment indicating that the classical equations used are valid even when the rate at which the temperature is changing is as high as 10^{10} degrees per second. All of the experimental data can be satisfactorily explained by classical thermal considerations. Both the thermionic emission and the "reverse photoelectric effect" provide very sensitive means for monitoring the temperature variations of surfaces when the temperature is varying at such a rapid rate. Thermionic emission is extremely sensitive to temperature and may provide a very accurate method of high-

temperature monitoring during laser-beam-surface interactions. It is interesting to note that the equations for thermal conductivity and thermionic emission give reasonable results in the time intervals involved in these experiments.

We would like to express appreciation to Mr. Robert Oswald and Mr. Dick Linner for their aid in the experimental program and to the many members of the Research Center for helpful and stimulating discussions. Special thanks are due to Dr. R. B. McQuistan for persistent, searching, and illuminating questions.

[1]R. L. Smith, Phys. Rev. 128, 2225 (1962).
[2]I. Langmuir and H. A. Jones, Gen. Elec. Rev. 30, 408, 310, 354 (1927).
[3]J. F. Ready, Optical Society of America, 1963 Spring Meeting Program (unpublished), p. 11.

3.86-MeV LEVEL IN F^{17}†

R. E. Segel, P. P. Singh, R. G. Allas, and S. S. Hanna
Argonne National Laboratory, Argonne, Illinois
(Received 15 March 1963)

In a recent experiment, Broude, Alexander, and Litherland[1] have shown that the 3.85-MeV level in O^{17} probably has $J^{\pi}=\frac{5}{2}^-$ instead of the long-accepted value[2] of $\frac{7}{2}^-$. The latter assignment, along with some other evidence, had been taken[3] to indicate a "good" single-particle level described by the configuration $O^{16}(1f_{7/2})$. Since the assignment of $\frac{5}{2}^-$ to this state would have an important effect on the location and nature of the single-particle levels in the mass-17 nuclei, it was decided to re-examine the original assignment[4] of $\frac{7}{2}^-$ to the analog state in F^{17} at 3.86 MeV. There is considerable evidence to show that in both F^{17} and O^{17} the state is produced by the interaction of f-wave nucleons with O^{16}. This narrows the assignment to $\frac{7}{2}^-$ or $\frac{5}{2}^-$. Since the only evidence[4] for $\frac{7}{2}^-$, obtained from $O^{16}(p,p)O^{16}$, is not entirely conclusive,[5] a definitive assignment was sought in the radiative capture $O^{16}(p,\gamma)F^{17}$ which, as will appear, is ideal for this purpose.

Rotating targets[6] of Ta_2O_5 were irradiated with a 10-μA proton beam, $E_p=3.4$-3.5 MeV, and the resulting radiation was detected with a NaI crystal, 10 in. in diameter by 8 in. thick. The reaction was also monitored with a 4-×4-in. crystal. The only appreciable radiation observed above $E_\gamma=1.5$ MeV was at 5.3 MeV from $O^{18}(p,\alpha\gamma)N^{15}$, at 3.86 MeV primarily from resonant radiative capture to the ground state of F^{17} (the desired process), and at 3.36 MeV from direct capture to the first excited state. A spectrum is shown in Fig. 1. Yield curves for the 3.86-MeV radiation at $\theta=90°$ are illustrated in Fig. 2. The shape of the lower curve is taken to indicate a target thicker than the width of the resonance. With this target, angular distributions were obtained at $E_p=3.473$, 3.470, and 3.465 MeV[7] as depicted in Fig. 3.

The data were fitted with the expressions $A_0(1+\sum_1^N A_nP_n)$ with $N=1$-6. The coefficients (for $N=4$), corrected for the solid angle of the detector, are listed in Table I. At $E_p=3.473$ MeV, where the yield is integrated over the whole resonance, the angular distribution is very well represented by $1+A_2P_2(\theta)$ with $A_2=0.47\pm0.03$. Hence the radiation is almost pure dipole, and the assignment to the level is $\frac{5}{2}^-$, since the theoretical values are $A_2=-0.36$ and 0.46 for $\frac{7}{2}^-$ and $\frac{5}{2}^-$, respectively. If f-wave interaction is not assumed, the present result eliminates the assignments $\frac{1}{2}^{\pm}$, $\frac{3}{2}^{\pm}$, $\frac{7}{2}^{\pm}$, $\frac{9}{2}^{\pm}$, and higher spins. Since the angular distributions are insensitive to parity, the value

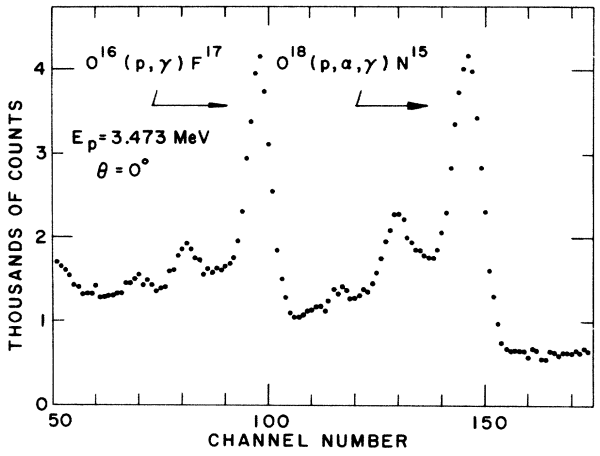

FIG. 1. NaI pulse-height spectrum for radiation emitted at 0° in proton bombardment ($E_p=3.473$ MeV) of a tantalum oxide target. The energy is 3.86 MeV for the resonant capture radiation.

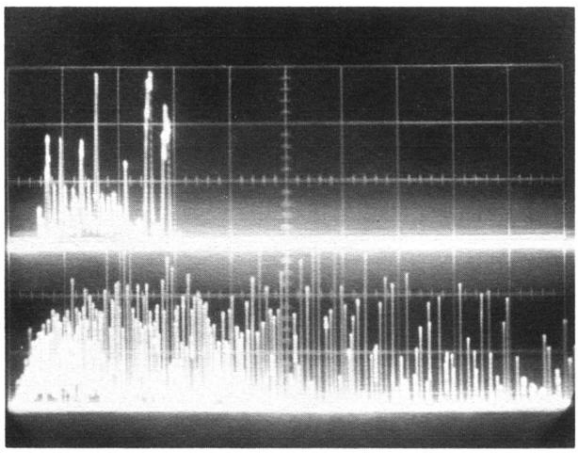

FIG. 2. Scope traces showing electron emission due to absorption of ruby laser beam by carbon target. Lower trace is output of ruby laser. Time scale is 50 μsec/cm. Upper trace shows electron emission pulses. Amplitude scale corresponds to 20 mA/cm. Collector is positive with respect to the target.

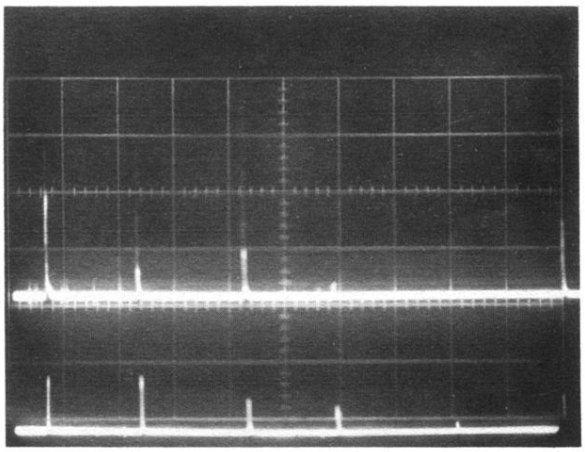

FIG. 3. Results of absorption of neodymium laser beam by carbon target. Lower trace shows output of the laser at 20 μsec/cm. Upper trace shows electron emission pulses. Amplitude calibration is 2 mA/cm. Collector is positive with respect to the target.

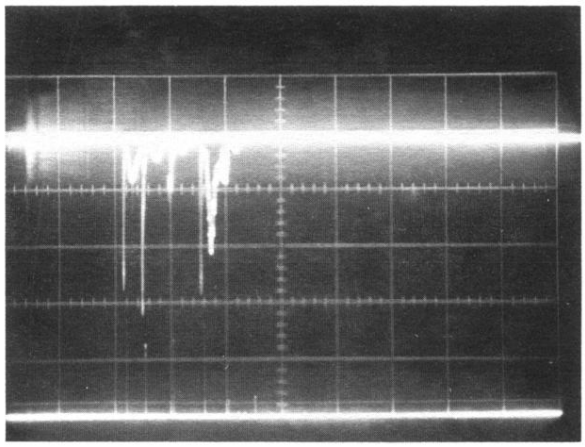

FIG. 5. Results of absorption of neodymium laser beam by the carbon target with the collector held negative with respect to the target. The time scale is 100 μsec/cm. The lower trace indicates the output of the laser. The upper trace indicates electrons arriving at the target. Amplitude scale is 100 μA/cm.